Inorg. Chem. **2007**, *46*, 6632–6639

Albumin Binding, Relaxivity, and Water Exchange Kinetics of the Diastereoisomers of MS-325, a Gadolinium(III)-Based Magnetic Resonance Angiography Contrast Agent

Peter Caravan,*,† Giacomo Parigi,¶ Jaclyn M. Chasse,† Normand J. Cloutier,† Jeffrey J. Ellison,† Randall B. Lauffer,† Claudio Luchinat,¶ Sarah A. McDermid,† Marga Spiller,‡ and Thomas J. McMurry†

EPIX Pharmaceuticals, 67 Rogers Street, Cambridge, Massachusetts 02142, CERM and Department of Agricultural Biotechnology, University of Florence, Via L. Sacconi 6, I-50019 Sesto Fiorentino, Italy, and Department of Radiology, New York Medical College, Valhalla, New York 10595

Received April 10, 2007

The amphiphilic gadolinium complex MS-325 ((trisodium-{(2-(*R*)-[(4,4-diphenylcyclohexyl) phosphonooxymethyl] diethylenetriaminepentaacetato) (aquo)gadolinium(III)}) is a contrast agent for magnetic resonance angiography (MRA). MS-325 consists of two slowly interconverting diastereoisomers, **A** and **B** (65:35 ratio), which can be isolated at pH > 8.5 (Tyeklár, Z.; Dunham, S. U.; Midelfort, K.; Scott, D. M.; Sajiki, H.; Ong, K.; Lauffer, R. B.; Caravan, P.; McMurry, T. J. *Inorg. Chem.* **2007**, *46*, 6621–6631). MS-325 binds to human serum albumin (HSA) in plasma resulting in an extended plasma half-life, retention of the agent within the blood compartment, and an increased relaxation rate of water protons in plasma. Under physiological conditions (37 °C, pH 7.4, phosphate buffered saline (PBS), 4.5% HSA, 0.05 mM complex), there is no statistical difference in HSA affinity or relaxivity between the two isomers (**A** 88.6 ± 0.6% bound, $r_1 = 42.0 \pm 1.0$ mM^{-1} s^{-1} at 20 MHz; **B** 90.2 ± 0.6% bound, $r_1 = 38.3 \pm 1.0$ mM^{-1} s^{-1} at 20 MHz; errors represent 1 standard deviation). At lower temperatures, isomer **A** has a higher relaxivity than isomer **B**. The water exchange rates in the absence of HSA at 298 K, $k_A^{298} = 5.9 \pm 2.8 \times 10^6$ s^{-1}, $k_B^{298} = 3.2 \pm 1.8 \times 10^6$ s^{-1}, and heats of activation, $\Delta H^{\ddagger}_A = 56 \pm 8$ kJ/mol, $\Delta H^{\ddagger}_B = 59 \pm 11$ kJ/mol, were determined by variable-temperature ^{17}O NMR at 7.05 T. Proton nuclear magnetic relaxation dispersion (NMRD) profiles were recorded over the frequency range of 0.01–50 MHz at 5, 15, 25, and 35 °C in a 4.5% HSA in PBS solution for each isomer (0.1 mM). Differences in the relaxivity in HSA between the two isomers could be attributed to the differing water exchange rates.

Introduction

The use of contrast agents in clinical magnetic resonance imaging (MRI) has become routine. The most widely used contrast agents are gadolinium(III) complexes.[1−3] The Gd-(III) complexes share the common feature of an octadentate ligand and one inner-sphere water molecule. In clinical MRI, water and fat are being imaged and contrast agents function by shortening the T_1 of water protons wherever the complex localizes. In a T_1-weighted MR image, water molecules with the shortest T_1 will give the largest signal. Consequently, areas of the body containing contrast agent will appear as bright regions in an MR image.

MS-325 is a commercial contrast agent (generic name gadofosveset, trade name Vasovist) approved in some countries to assess blockages in arteries.[4,5] MS-325 functions by reversibly binding to human serum albumin (HSA) in

* To whom correspondence should be addressed. Current address: Athinoula A. Martinos Center for Biomedical Imaging, Department of Radiology, Massachusetts General Hospital, Charlestown, MA 02129. E-mail: caravan@nmr.mgh.harvard.edu. Fax: 617-726-7422.
† EPIX Pharmaceuticals.
¶ University of Florence.
‡ New York Medical College.

(1) Caravan, P.; Ellison, J. J.; McMurry, T. J.; Lauffer, R. B. *Chem. Rev.* **1999**, *99*, 2293−2352.
(2) Caravan, P.; Lauffer, R. B., Contrast Agents: Basic Principles. In *Clinical Magnetic Resonance Imaging*, 3rd ed.; Edelman, R. R., Hesselink, J. R., Zlatkin, M. B., Crues, J. V., Eds.; Saunders: Philadelphia, 2005; Vol. 1, pp 357−375.
(3) Merbach, A. E., Toth, E., Eds. *The Chemistry of Contrast Agents in Medical Magnetic Resonance Imaging*; Wiley: New York, 2001.

10.1021/ic700686k CCC: $37.00
Published on Web 07/11/2007

Chart 1. Complexes Used in This Study

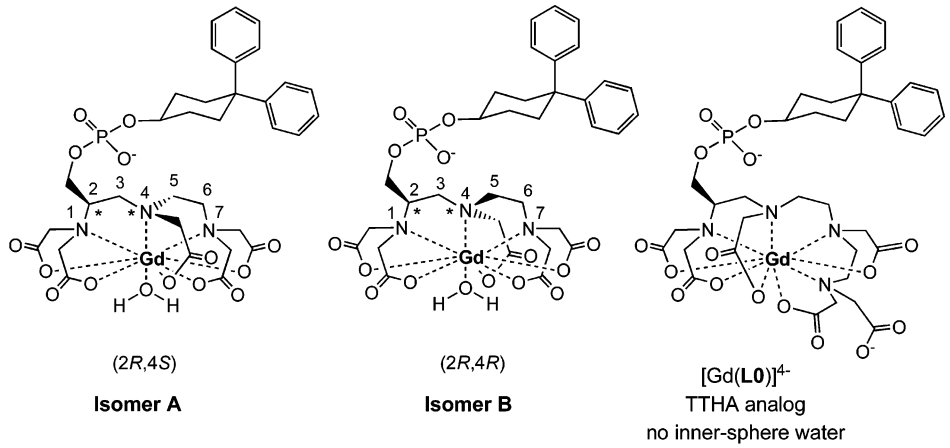

plasma.[6,7] Binding to HSA helps to keep the complex in the plasma compartment and extends the circulating time of the complex resulting in better delineation of blood vessels and the ability to perform high-resolution imaging in multiple body regions. In addition, binding to HSA serves to slow the rotation of the complex. As the rotational diffusion rate of the complex becomes closer to the proton Larmor frequency, the efficacy of MS-325 as a contrast agent increases. The efficiency of contrast agents is defined as relaxivity, r_1, the degree to which a given concentration can change $1/T_1$

$$r_1 = \frac{\Delta(1/T_1)}{[\mathrm{Gd}]} \qquad (1)$$

The relaxivity of MS-325 is enhanced up to 9-fold in HSA compared to MS-325 in buffer alone (without HSA).

In a companion paper,[8] it was demonstrated that MS-325 exists as a pair of interconverting isomers in a 1.8:1 ratio (Chart 1). There are two chiral centers in the complex: the methine carbon, 2, and the central amine nitrogen. MS-325 is synthesized from L-serine resulting in an *R* configuration at carbon 2, but the central nitrogen can adopt *R* or *S* chirality. In addition, there are two possible wrapping isomers formed, whereby the ligand wraps about the ion in a right- (Δ) or left-handed (Λ) turn. This results in four possible diastereomers: $\Delta R,R$, $\Delta R,S$, $\Lambda R,R$, $\Lambda R,S$. However, only the Λ diasteromers, $\Lambda R,R$ and $\Lambda R,S$, are observed because the Δ configuration requires the large albumin binding moiety to occupy the energetically disfavored axial position on the chelate ring. The $\Lambda R,S$ species was denoted isomer **A** (elutes earlier, more prevalent), and the $\Lambda R,R$ was denoted isomer **B**. The name "MS-325" refers to the sodium salt of the equilibrated isomer mixture. The purpose of this paper is to determine if there is any difference in efficacy between the two isomers. To this end, we report HSA-binding studies at various complex/protein ratios, probe displacement studies to identify the region on HSA where the isomers bind, relaxivity studies as a function of field and temperature in the presence and absence of HSA, and variable-temperature ^{17}O NMR studies to ascertain the water exchange rates at the two isomers.

Experimental Section

Materials. The **A** (>97.5% isomerically pure) and **B** (>99.2% isomerically pure) isomers were isolated as described previously.[8] Na_4[Gd(**L0**)] was prepared as described.[6] Human serum albumin (HSA), product number A-1653 (Fraction V Powder 96−99% albumin, containing fatty acids), HSA absorbance standards, and the fluorescent probes, dansyl L-asparagine (DNSA) and dansylsarcosine piperidinium salt (DS), were purchased from Sigma Chemical Company (St. Louis, Mo.). Ultrafiltration units (UFC3LCC00, regenerated cellulose membrane of 5000 Dalton nominal molecular weight cutoff) were obtained from Millipore Corporation, Bedford, MA. Other reagents were supplied by Aldrich Chemical Co., Inc., and were used without further purification.

Ultrafiltration Measurements of Binding. Solutions containing a clinically relevant concentration (0.05, 0.10, 0.50, and 1.2 mM) of Gd chelate and HSA (4.5% w/v) were prepared by addition of an appropriate volume of MS-325 drug product, isomer **A**, or isomer **B** stock solution and PBS (such that the total added volume was 144 μL) to a vial containing 5000 μL of 4.63% HSA, such that the resultant solution is 4.50% HSA. The solutions were mixed, and 10 aliquots (400μL) of these samples were placed in 5 kDa ultrafiltration units. Two additional 25 μL aliquots were analyzed by ICP-MS to determine the total Gd concentration. The samples were incubated at 37 °C for 10 min and then centrifuged at 5800 g for 3.5 min. The filtrates (~30 μL) from these ultrafiltration units were used to determine the free concentration of complex in each of the samples by ICP-MS.

(4) Goyen, M.; Edelman, M.; Perreault, P.; O'Riordan, E.; Bertoni, H.; Taylor, J.; Siragusa, D.; Sharafuddin, M.; Mohler, E. R.; Breger, R.; Yucel, E. K.; Shamsi, K.; Weisskoff, R. M. *Radiology* **2005**, *236*, 825−33.
(5) Rapp, J. H.; Wolff, S. D.; Quinn, S. F.; Soto, J. A.; Meranze, S. G.; Muluk, S.; Blebea, J.; Johnson, S. P.; Rofsky, N. M.; Duerinckx, A.; Foster, G. S.; Kent, K. C.; Moneta, G.; Middlebrook, M. R.; Narra, V. R.; Toombs, B. D.; Pollak, J.; Yucel, E. K.; Shamsi, K.; Weisskoff, R. M. *Radiology* **2005**, *236*, 71−8.
(6) Caravan, P.; Cloutier, N. J.; Greenfield, M. T.; McDermid, S. A.; Dunham, S. U.; Bulte, J. W. M.; Amedio, J. C., Jr.; Looby, R. J.; Supkowski, R. M.; Horrocks, W. D., Jr.; McMurry, T. J.; Lauffer, R. B. *J. Am. Chem. Soc.* **2002**, *124*, 3152−3162.
(7) Lauffer, R. B.; Parmelee, D. J.; Dunham, S. U.; Ouellet, H. S.; Dolan, R. P.; Witte, S.; McMurry, T. J.; Walovitch, R. C. *Radiology* **1998**, *207*, 529−538.
(8) Tyeklár, Z.; Dunham, S. U.; Midelfort, K.; Scott, D. M.; Sajiki, H.; Ong, K.; Lauffer, R. B.; Caravan, P.; McMurry, T. J. *Inorg. Chem.* **2007**, *46*, 6621−6631.

Determination of Site-Specific Binding Constants. This was done as described previously[9] using a Perkin-Elmer HTS-7000+ fluorescence plate reader. The affinities of the fluorescent probes for albumin were as follows: DS, $K_d = 5.0\ \mu$M, and DNSA, $K_d = 14.0\ \mu$M. Eight solutions containing [fluorescent probe] $\approx$ [HSA] $\approx K_d$ and ranging from 0 to 400 μM MS-325 isomer were prepared, and the fluorescence was measured in quadruplicate in 96-well plates. The fluorescence of HSA in PBS was measured to determine the minimum fluorescent intensity.

The fractional drop in fluorescence at a particular isomer concentration was interpreted as a fractional displacement of the bound fluorescent probe. The observed fluorescence was converted to a concentration of fluorescent probe bound to HSA, $[FP]_{bound}$. The concentration of bound probe is also given by eq 2, where K_d^{app} is the apparent dissociation constant of the probe in the presence of an isomer and is related to K_d by eq 3. K_i represents the site specific dissociation constant for a given isomer. The $[FP]_{bound}$ measured from fluorescence was compared to $[FP]_{bound}$ calculated using eqs 2 and 3. The sum of squares of the differences between the two was minimized by iteratively varying K_i, the initial fluorescence ($\pm$15%, this represented the scatter in the initial fluorescence and took into account any changes in solution composition upon adding isomer), and the fluorescence in the absence of the probe, total displacement ($\pm$15%).

$$[FP]_{bound} = \frac{([HSA]_t + [FP]_t + K_d^{app}) - \sqrt{([HSA]_t + [FP]_t + K_d^{app})^2 - 4[HSA]_t[FP]_t}}{2} \quad (2)$$

$$K_d^{app} = K_d\left(1 + \frac{[MS\text{-}325]_{free}}{K_i}\right) \quad (3)$$

Relaxivity. Relaxivities were determined at 20 (0.47 T) and 64.5 MHz (1.5 T) using a Bruker NMS 120 Minispec and a modified Varian XL-300, respectively. T_1 was measured with an inversion recovery pulse sequence, and all samples were measured at 37 °C. The ^{1}H NMRD profiles (5, 15, 25, and 35 °C) were recorded on a field cycling relaxometer at NY Medical College over the frequency range of 0.01−50 MHz. Twenty-two data point dispersions were recorded at each temperature. Aliquots were taken after each temperature measurement and analyzed by HPLC to ensure that there was minimal (<5%) isomerization during the study.

^{17}O NMR. $H_2{}^{17}O$ transverse relaxation rates were determined for a PBS buffer solution in the presence and absence of 11.45 m*m* isomer **A** or 13.12 m*m* isomer **B** as a function of temperature (−5 to 55 °C) on a Varian Unity 300 NMR operating at 40.6 MHz. Probe temperatures were determined from ethylene glycol or methanol chemical shift calibration curves. T_2 was determined by a CPMG pulse sequence. Aliquots were taken after each temperature measurement and analyzed by HPLC to ensure that there was minimal (<5%) isomerization during the study.

Results and Discussion

Albumin Binding. The binding of each isomer to HSA was studied at four concentrations by equilibrium ultracentrifugation. In addition to isomers **A** and **B**, the equilibrated isomer mixture, MS-325, was also studied under the same conditions. The binding data are summarized in Table 1. The binding is similar between both isomers. Isomer **B** has a tendency to higher affinity at all the concentrations studied; however this is not a significant difference. The binding data reported here are in excellent agreement with that reported earlier for MS-325.[6]

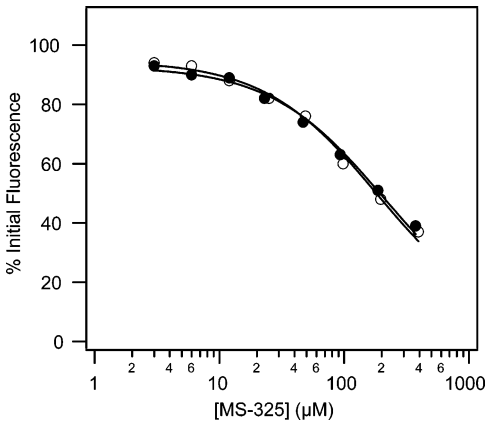

Figure 1. Displacement of site II probe dansylsarcosine from HSA by isomers **A** (●) and **B** (○) of MS-325.

Table 1. Equilibrium Binding for MS-325 (fully Equilibrated Mixture), **A**, and **B** to 4.5% HSA at 37 °C in PBS[a]

total concentration (mM)	% bound equilibrated MS-325	% bound **A**	% bound **B**
0.050	88.4 (0.6)	88.6 (0.6)	90.2 (0.6)
0.10	86.9 (0.6)	87.2 (0.7)	88.9 (1.0)
0.50	76.7 (0.7)	77.0 (1.5)	78.4 (1.3)
1.20	60.9 (1.0)	61.7 (1.2)	63.7 (1.8)

[a] Numbers in parentheses represent 1 standard deviation.

Table 2. Inhibition Constants for Isomers **A** and **B** at 37 °C in PBS for the Displacement of Dansylsarcosine (DS) or Dansylasparagine (DNSA) from HSA[a]

sample	K_i (μM) DS	K_i (μM) DNSA
isomer **A**	85 (20)	1700 (1100)
isomer **B**	76 (17)	740 (185)
equilibrated MS-325	85 (1)	1500 (300)

[a] Numbers in parentheses represent 1 standard deviation.

The ability of each isomer to displace site-specific fluorescent probes was also studied. Dansyl-L-asparagine (DNSA) was used as a probe for binding site I on subdomain IIA. Dansylsarcosine (DS) was used to probe the binding of each isomer to binding site II on subdomain IIIA. These probes fluoresce when bound to HSA. Isomer **A** or **B** was added to a solution containing a fluorescent probe, and the change in fluorescence was monitored. A decrease in fluorescence was taken as displacement of the probe by the isomer. Both isomers significantly displace DS (Figure 1) but only weakly displace DNSA suggesting that the isomers bind to the same location on HSA, site II. The inhibition constants, K_i, for probe displacement are given in Table 2. The magnitude of the DS inhibition constant is in good agreement with equilibrium binding studies. For instance, if one converts the K_i values into percent bound under the conditions 0.050 mM isomer and 0.66 mM HSA, then one arrives at 88.0 and 89.3% bound for isomers **A** and **B**, respectively. This suggests that at low concentrations of Gd complex, either isomer will be primarily bound to site II.

(9) Caravan, P.; Cloutier, N. J.; Greenfield, M. T.; McDermid, S. A.; Dunham, S. U.; Bulte, J. W.; Amedio, J. C., Jr.; Looby, R. J.; Supkowski, R. M.; Horrocks, W. D., Jr.; McMurry, T. J.; Lauffer, R. B. *J. Am. Chem. Soc.* **2002**, *124*, 3152−62.

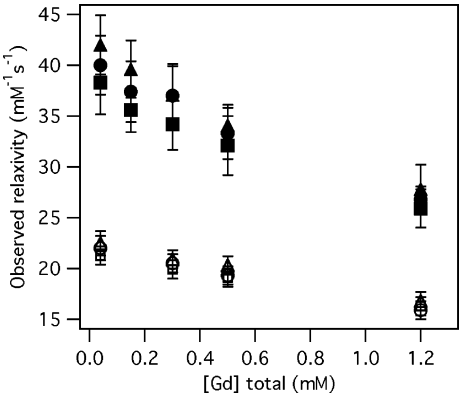

Figure 2. Effect of Gd:HSA ratio (0.67 mM HSA) on relaxivity for isomer **A** (▲, △), isomer **B** (■, □), and equilibrated MS-325 (●, ○) at 0.47 T = 20 MHz (▲, ■, ●) and 1.5 T = 64 MHz (△, □, ○).

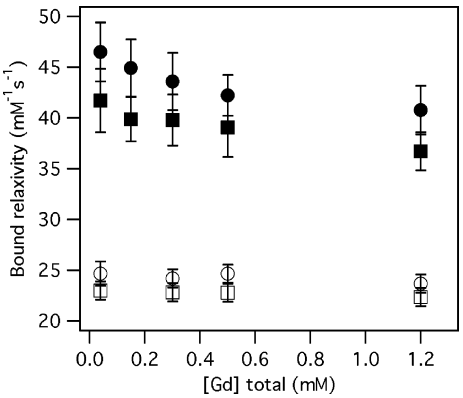

Figure 3. Mean bound relaxivity, $\bar{r}_{1b}$, for isomers **A** (●, ○) and **B** (■, □) bound to HSA at 0.47 T (●, ■) and 1.5 T (○, □).

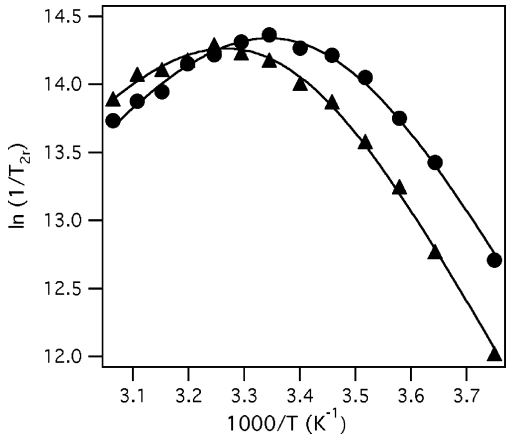

Figure 4. Variable-temperature transverse relaxation of $H_2{}^{17}O$ in the presence of isomer **A** (●) or **B** (▲). At low temperatures, the system approaches slow exchange ($1/T_{2r} \approx k_{ex}$) and shows that water exchange is faster at isomer **A**.

Relaxivity. Relaxivities were determined at two field strengths (0.47 T = 20 MHz and 1.5 T = 64 MHz). There is a large body of relaxivity data at 0.47 T with which to compare, but 1.5 T is a more clinically relevant field strength for MRI contrast agents. In the absence of albumin, the relaxivities are the same among the isomers and the equilibrated MS-325, Table 3. Typically relaxivities are determined by measuring the relaxation rate as a function of concentration and then taking the slope from a plot of relaxation rate versus concentration. Since MS-325 is only moderately bound to albumin, the relative amounts of bound and free complex will depend on the concentration, and hence the observed relaxivity will be concentration dependent. Multiple samples were prepared at a given concentration of MS-325, isomer **A**, or isomer **B** (0.04, 0.15, 0.3, 0.5, and 1.2 mM) and a fixed concentration of HSA (4.5%, pH 7.4, 37 °C). Relaxivities were calculated using eq 1 by subtracting the relaxation rate of HSA from that of HSA + complex and dividing the result by concentration. The relaxivities are plotted in Figure 2. As expected the observed relaxivity falls off with increased concentration because the fraction bound to albumin decreases. Isomer **A** has a slightly higher relaxivity than isomer **B** at all concentrations studied. The equilibrated mixture of the two is intermediate.

Table 3. Relaxivities in Phosphate Buffered Saline (PBS), 37 °C at Two Magnetic Field Strengths (Proton Frequencies)[a]

sample	r_{1f} (mM^{-1} s^{-1}) 20 MHz	r_{1f} (mM^{-1} s^{-1}) 64 MHz
equilibrated MS-325	6.84 (0.48)	5.47 (0.39)
isomer **A**	6.91 (0.49)	5.66 (0.40)
isomer **B**	6.86 (0.49)	5.73 (0.41)

[a] Numbers in parentheses represent 1 standard deviation.

The relative fraction of bound and free is known at each concentration. The relaxivity in the absence of HSA was determined, r_{1f} (see Table 3). The mean relaxivity resulting from the bound fraction, $\bar{r}_{1b}$, can be calculated from eq 4 where $R_1{}^{obs}$ and $R_1{}^{dia}$ are the relaxation rates measured in the presence and absence of MS-325

$$\bar{r}_{1b} = \frac{(R_1{}^{obs} - R_1{}^{dia} - [\text{MS-325}]_f \times r_{1f})}{[\text{MS-325}]_b} \qquad (4)$$

The bound relaxivities for each isomer are summarized in Figure 3. Two things are apparent from Figure 3: the bound relaxivity for **A** is greater than the bound relaxivity for B at all concentrations, and the bound relaxivity for each isomer decreases slightly with increasing concentrations. The decrease in bound relaxivity with increasing concentration may be indicative of different binding sites having somewhat different relaxivities. It appears that the weaker binding sites are sites of lower relaxivity.

Water Exchange. It is known that for lanthanide complexes of DOTA and its derivatives that there exist interconverting conformational isomers (capped square antiprism and twisted capped square antiprism).[10−13] It was elegantly shown that the water exchange rates between these conformational isomers can vary by 2 orders of magnitude.[14−16] Burai et al.[17] recently reported water exchange rates for diastereomers of $[Gd(NH_2\text{-bz-DTPA})(H_2O)]^{2-}$. For this DTPA derivative, the difference in water exchange rate was only a factor of 2.

The water exchange rate was directly probed by measuring the transverse relaxation rates of $H_2{}^{17}O$ water as a function of temperature for each isomer. The data are plotted in Figure 4. For Gd(III) complexes, where the paramagnetic chemical shift of $H_2{}^{17}O$ is small, the reduced transverse relaxation rate ($1/T_{2r}$) of bulk $H_2{}^{17}O$ is given by eq 5

$$\frac{1}{T_{2r}} = \left(\frac{1}{T_2} - \frac{1}{T_{2A}}\right)\left(\frac{[H_2O]}{q[Gd]}\right) = \frac{1}{T_{2m} + \tau_m} \quad (5)$$

where T_{2A} refers to the relaxation rate of the diamagnetic reference and q is the number of water molecules coordinated to each gadolinium(III) ion. At high temperatures, $1/T_{2r} \approx 1/T_{2m}$, while at low temperatures (slow exchange condition), $1/T_{2r} \approx 1/\tau_m = k_{ex}$. At the low-temperature extreme in Figure 4, it is clear that $1/T_{2r}$ and, hence k_{ex}, is greater for isomer **A** than for **B**.

The relaxation mechanism for $1/T_{2m}$ is predominantly scalar; $1/T_{2m}$ is a function of T_{1e} (the electronic relaxation time of Gd(III), denoted here as $T_{1e}{}^{HF}$ for "high field"), τ_m, and the hyperfine coupling constant, $A/\hbar$, between the Gd ion and the oxygen nucleus, eq 6, where S is the spin quantum number ($S = 7/2$) for Gd(III).

$$\frac{1}{T_{2m}} \approx \frac{1}{T_2{}^{scalar}} = \frac{S(S+1)}{3}\left(\frac{A}{\hbar}\right)^2 \tau_{sc}; \frac{1}{\tau_{sc}} = \frac{1}{T_{1e}} + \frac{1}{\tau_m} \quad (6)$$

$$\frac{1}{\tau_m} = k_{ex} = \frac{k_B T}{h}\exp\left[\frac{\Delta S^{\ddagger}}{R} - \frac{\Delta H^{\ddagger}}{RT}\right] = \frac{k_{ex}^{298} T}{298.15}\exp\left[\frac{\Delta H^{\ddagger}}{R}\left(\frac{1}{298.15} - \frac{1}{T}\right)\right] \quad (7)$$

$$\frac{1}{T_{1e}{}^{HF}} = \frac{1}{T_{1e}{}^{298}}\exp\left[\frac{\Delta E_{T1e}}{R}\left(\frac{1}{T} - \frac{1}{298.15}\right)\right] \quad (8)$$

Values for $A/\hbar$ for oxygen coordinated to a lanthanide fall in a narrow range;[18] Merbach and co-workers[19] have shown that $A/\hbar$ for water coordinated to Gd(III) is typically -3.8×10^6 rad/s, and this value was assumed here. The electronic relaxation rate, $1/T_{1e}$, and k_{ex} were assumed to have exponential temperature dependence. The ^{17}O relaxation rate data were fit to four parameters: $k_{ex}{}^{298}$ (water exchange rate at 298 K), $\Delta H^{\ddagger}$ (enthalpy of activation), $1/T_{1e}{}^{298}$ (electronic relaxation rate at 298 K), and ΔE_{T1e} (activation energy for $1/T_{1e}$). The results are summarized in Table 4. Water exchange is faster at isomer **A** by about a factor of 2. The activation activation enthalpies are very similar, implying that the difference in water exchange is a difference in the entropy of activation. The water exchanges rates are virtually identical to those reported for the diastereomers of $[Gd(NH_2\text{-bz-DTPA})(H_2O)]^{2-}$.[17]

Table 4. Water Exchange and Electronic Relaxation Parameters for Isomers **A** and **B** in PBS in the Absence of Albumin (7.05 T)[a]

	isomer **A**	isomer **B**
$\tau_m{}^{308}$ (ns)	79 (37)	140 (74)
$k_{ex}{}^{298}$ ($\times 10^6$ s^{-1})	5.9 (2.8)	3.2 (1.8)
$\Delta H^{\ddagger}$ (kJ mol^{-1})	56 (8)	59 (11)
$1/T_{1e}{}^{298}$ ($\times 10^7$ s^{-1})	2.7 (0.4)	2.7 (0.4)
ΔE_{T1e} (kJ mol^{-1})	−12.7 (2.3)	−12.7 (2.3)

[a] Numbers in parentheses represent 1 standard deviation.

^{1}H NMRD. The differences in water exchange rates imply that the proton relaxivities of the two isomers in HSA solution should be different and that this difference should be greater at low temperatures, provided the water exchange rates do not change when the complex is bound to albumin. Relaxivity is the change in the relaxation rate of solvent water protons normalized to metal ion concentration (in mM) and expressed in units of mM^{-1} s^{-1}. Relaxivity can be factored into two components: inner sphere, resulting from relaxation enhancement caused by the inner-sphere coordinated water molecule exchanging with the bulk, and outer sphere, which comprises the contributions of water molecules in the second coordination sphere and diffusion of water near the ion, eq 6

$$r_1 = r_1{}^{IS} + r_1{}^{OS} = \frac{q/[H_2O]}{T_{1m} + \tau_m} + r_1{}^{OS} \quad (9)$$

Here, q is the number of inner-sphere water molecules, $[H_2O]$ is the water concentration in mM (typically 55 600 mM), T_{1m} is the relaxation time of the coordinated inner-sphere water protons, and τ_m is the lifetime of this water (the water exchange rate, $k_{ex} = 1/\tau_m$). Inspection of eq 9 indicates that slow water exchange will limit relaxivity provided τ_m is comparable to, or larger than T_{1m}. Limitation of relaxivity by slow water exchange should be most evident at low temperatures because τ_m increases with decreasing temperature, while T_{1m} typically decreases with temperature as rotational diffusion slows. Provided that T_{1m} and $r_1{}^{OS}$ are the same for both isomers, one would expect relaxivity differences between the isomers to be largest at low temperatures, where the slow exchange limit is approached ($\tau_m > T_{1m}$), and differences in water exchange rates dominate observed relaxivity.

To further investigate this, NMRD profiles were recorded at four temperatures (5, 15, 25, and 35 °C) for isomer **A**, isomer **B**, and $[Gd(\mathbf{L0})]^{4-}$ (Chart 1) in HSA solution. Studies were carried out under conditions where the protein (0.67 mM) is in significant excess to the metal complex (0.085

(10) Aime, S.; Botta, M.; Ermondi, G. *Inorg. Chem.* **1992**, *31*, 4291−9.
(11) Desreux, J. F. *Inorg. Chem.* **1980**, *19*, 1319−24.
(12) Hoeft, S.; Roth, K. *Chem. Ber.* **1993**, *126*, 869−73.
(13) Jacques, V.; Desreux, J. F. *Inorg. Chem.* **1994**, *33*, 4048−53.
(14) Aime, S.; Barge, A.; Bruce, J. I.; Botta, M.; Howard, J. A. K.; Moloney, J. M.; Parker, D.; de Sousa, A. S.; Woods, M. *J. Am. Chem. Soc.* **1999**, *121*, 5762−5771.
(15) Dunand, F. A.; Aime, S.; Merbach, A. E. *J. Am. Chem. Soc.* **2000**, *122*, 1506−1512.
(16) Woods, M.; Aime, S.; Botta, M.; Howard, J. A. K.; Moloney, J. M.; Navet, M.; Parker, D.; Port, M.; Rousseaux, O. *J. Am. Chem. Soc.* **2000**, *122*, 9781−9792.
(17) Burai, L.; Toth, E.; Sour, A.; Merbach, A. E. *Inorg. Chem.* **2005**, *44*, 3561−3568.
(18) Peters, J. A.; Huskens, J.; Raber, D. J. *Prog. Nucl. Magn. Reson. Spectrosc.* **1996**, *28*, 283−350.
(19) Powell, D. H.; Ni Dhubhghaill, O. M.; Pubanz, D.; Helm, L.; Lebedev, Y. S.; Schlaepfer, W.; Merbach, A. E. *J. Am. Chem. Soc.* **1996**, *118*, 9333−9346.

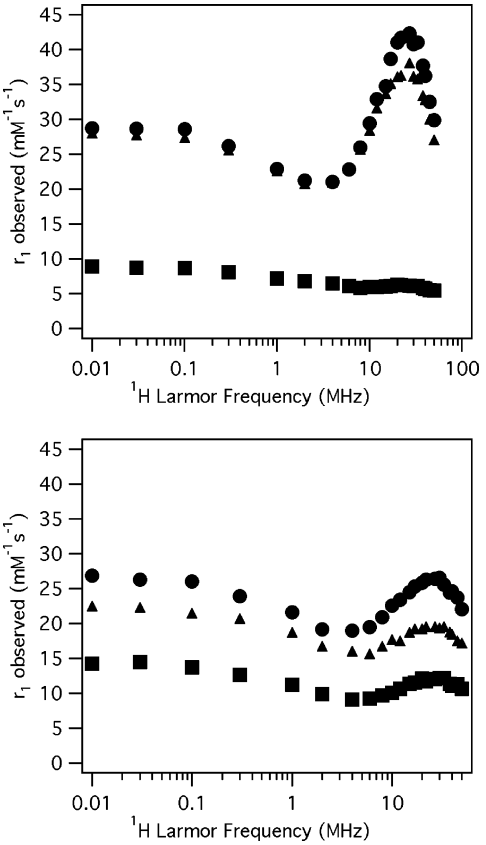

Figure 5. ^{1}H NMRD expressed as observed relaxivity of isomer **A** (●), isomer **B** (▲), or [Gd(**L0**)]$^{4-}$ (■) in 4.5% HSA solution at 35 (top) and 5 °C (bottom).

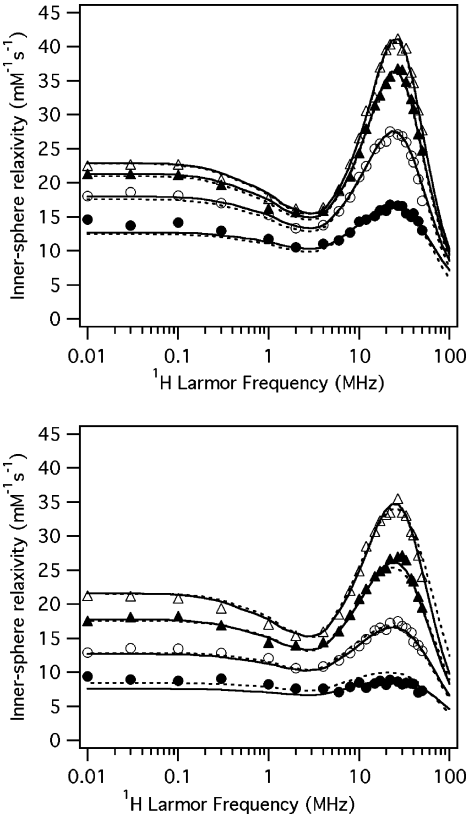

Figure 6. Inner-sphere relaxivity for isomers **A** (top) and **B** (bottom) bound to HSA at 35 (△), 25 (▲), 15 (○), and 5 (●) °C. Dashed and solid lines are fits using the isotropic and anisotropic models, respectively, with parameters from Table 5.

mM) to ensure that the complex is predominantly protein bound. Under these conditions, the fraction of isomer **A**, isomer B, and [Gd(**L0**)]$^{4-}$ bound to HSA was 88, 90, and 95%, respectively, and these numbers did not vary significantly over the temperature range studied. For the isomers of MS-325, luminescence studies demonstrated that $q = 1$.[8] [Gd(**L0**)]$^{4-}$ is derived from the TTHA ligand and was shown to contain no inner-sphere water.[6]

We define r_1^{obs} as observed relaxivity, which is the aggregate relaxivity of free and protein-bound components and is calculated by eq 1. Observed relaxivity is a useful practical measure for the comparison of different compounds that may differ in fraction bound or in protein-bound relaxivity. The observed NMRD relaxivity data (r_1^{obs} for 0.085 mM Gd, 0.67 mM HSA) are shown in Figure 5 for isomer **A**, isomer **B**, and [Gd(**L0**)]$^{4-}$ at 5 and 35 °C. At 35 °C, the relaxivities of isomers **A** and **B** are very similar at all frequencies, and these relaxivities are much greater than those of [Gd(**L0**)]$^{4-}$, which has no inner-sphere water. At 5 °C, the relaxivities of isomers **A** and **B** are much lower, and the high-field peak has become flatter. The relaxivity of isomer **A** is now clearly greater than that of isomer **B**. While the relaxivities of **A** and **B** decreased, the relaxivity of [Gd(**L0**)]$^{4-}$ is increased at low temperature, consistent with relaxation not limited by slow exchange. Since the fraction bound of these three complexes is quite high, the difference between the observed relaxivity of the isomers and [Gd(**L0**)]$^{4-}$ is a good estimate of the inner-sphere relaxivity. Figure 5 clearly shows that for this temperature range, the isomers are approaching the slow exchange limit. As the temperature is lowered, the contribution to r_1^{obs} from r_1^{IS} drops from 85 to 53% for **A** and from 83 to 37% for **B** (20 MHz going from 35 to 5 °C).

To assess the effect of the inner-sphere water of the isomers on relaxivity, it is assumed that the relaxivity of [Gd(**L0**)]$^{4-}$ when bound to albumin represents the outer- and second-sphere contributions to relaxivity of **A** and **B**. [Gd(**LO**)]$^{4-}$ has similar structure and charge (4- vs 3-) as **A** and **B** and binds to the same site on HSA. The inner-sphere relaxivity of either **A** or **B** is calculated by first calculating the bound relaxivity (eq 4) at each frequency and then subtracting the bound relaxivity of [Gd(**L0**)]$^{4-}$ at that frequency. This results in the calculated r_1^{IS} NMRD values that are plotted in Figure 6.

The data in Figure 6 were modeled in three ways. First, only higher-field data were considered ($\nu_H \geq 4$ MHz). Here it was assumed that the contribution to electronic relaxation from the static zero-field splitting (ZFS) was negligible and the data were fit to the Solomon−Bloembergen−Morgan equations.[20,21] At these proton frequencies, the contribution to relaxation dependent on the electronic Larmor frequency,

(20) Bertini, I.; Luchinat, C.; Parigi, G. *Adv. Inorg. Chem.* **2005**, *57*, 105−172.
(21) Kowalewski, J.; Kruk, D.; Parigi, G. *Adv. Inorg. Chem.* **2005**, *57*, 41−104.

ω_s, has dispersed, and the relaxation of the inner-sphere water is given by eq 10.

$$\frac{1}{T_{1m}} = \frac{2}{15}\left(\frac{\mu_0}{4\pi}\right)^2 \frac{\gamma_H{}^2 g_e{}^2 \mu_B{}^2 S(S+1)}{r_{GdH}{}^6}\left[\frac{3\tau_c}{1+\omega_H{}^2\tau_c{}^2}\right] \quad (10)$$

$$\frac{1}{T_{1e}} = \frac{\Delta_t{}^2[4S(S+1)-3]}{25}\left[\frac{\tau_v}{1+\omega_s{}^2\tau_v{}^2} + \frac{4\tau_v}{1+4\omega_s{}^2\tau_v{}^2}\right] \quad (11)$$

$$\tau_v = \tau_v{}^{308}\exp\left[\frac{\Delta E_v}{R}\left(\frac{1}{T} - \frac{1}{308.15}\right)\right] \quad (12)$$

$$\tau_R = \tau_R{}^{308}\exp\left[\frac{\Delta E_R}{R}\left(\frac{1}{T} - \frac{1}{308.15}\right)\right] \quad (13)$$

Here the correlation time, τ_c, has contributions from the electronic relaxation function and from rotational diffusion ($1/\tau_c = 1/T_{1e} + 1/\tau_R$), ω_H is the Larmor frequency of the proton (rad/s), γ_H is the proton magnetogyric ratio, g_e is the electronic g factor ($g_e = 2$ for Gd(III)), μ_B is the Bohr magneton, and μ_0 is the permittivity of vacuum. The mechanism for electronic relaxation is believed to be transient distortions resulting in zero-field splitting (ZFS) modulation and has a field dependence described by eq 11 where Δ_t is the magnitude of this transient ZFS, τ_v is a correlation time for these distortions, and ω_S is the Larmor frequency of the electron. It is assumed that the correlation times have exponential temperature dependencies (eqs 12 and 13). The Gd−H distance, r_{GdH}, was fixed to 3.1 Å as determined by an ENDOR study.[22] The high-field peak in Figure 6 arises because of the dispersion of the electronic relaxation rate. As the field increases, $1/T_{1e}$ becomes slower resulting in increased proton relaxation. At the peak of relaxivity, the condition $\omega_H{}^2\tau_c{}^2 > 1$ occurs, and relaxivity begins to decrease with increasing proton frequency.

This simple model reproduced the data reasonably well, but it was clear that there were some systematic deviations from the observed data. For instance this model predicts 35 °C relaxivities that are too high at the highest fields used. The effect of anisotropic relaxation was then examined by modifying the spectral density term after Lipari and Szabo[23] (eq 14)

$$\frac{1}{T_{1m}} = \frac{2}{15}\left(\frac{\mu_0}{4\pi}\right)^2 \frac{\gamma_H{}^2 g_e{}^2 \mu_B{}^2 S(S+1)}{r_{GdH}{}^6}\left[\frac{3F^2\tau_c}{1+\omega_H{}^2\tau_c{}^2} + \frac{3(1-F^2)\tau_f}{1+\omega_H{}^2\tau_f{}^2}\right] \quad (14)$$

where τ_f is a correlation time that takes into account fast local motion ($1/\tau_f = 1/\tau_c + 1/\tau_l$) and τ_l is a correlation time for fast motion; F^2 is an order parameter (often denoted S^2, but here F is used to avoid confusion with the spin quantum number) representing the degree of anisotropy ($F^2 = 1$ is an isotropic system). This modification had a dramatic effect on the quality of the fit (the sum of squares of residuals was reduced about 5-fold). For both isomers, a relatively large order parameter was obtained ($F^2 = 0.63$), and the fast correlation time was too short to be determined ($\tau_l < 100$ ps).

Table 5. NMRD Parameters for Isotropic and Anisotropic Fits of the $r_1{}^{IS}$ Data for Isomers **A** and **B** at 5, 15, 25, and 35 °C When Bound to Albumin

	isotropic fit		anisotropic fit	
	isomer **A**	isomer **B**	isomer **A**	isomer **B**
$\tau_R{}^{308}$ (ns)	5.0	4.6	4.9	4.9
ΔE_R (kJ/mol)	26	26	8.5	8.5
$\tau_m{}^{308}$ (ns)	198	296	67	182
$\Delta H^{\ddagger}$ (kJ/mol)	31	38	55	51
$\tau_v{}^{308}$ (ps)	20	22	16	16
ΔE_v (kJ/mol)	1.1	1.2	1.5	1.5
Δ_t (cm^{-1})	0.0147	0.0135	0.0128	0.0122
D (cm^{-1})	0.024	0.024	0.024	0.024
θ (deg)	37	41	50	51
F^2	1	1	0.63	0.67
τ_{fast} (ns)	NA	NA	<0.3	<0.3

Estimated errors are ±20%.

For a more rigorous analysis, the model developed by the Florence and Stockholm groups was used.[24,25] This model can take into account the effect of both static and transient ZFS on relaxation provided that the system is in the slow motion limit (i.e., the rotational correlation time is larger than the electron relaxation time) and within the Redfield limit, as in the present case.[26] In these cases it provides results in agreement with the general slow motion theory.[27] The static ZFS is introduced through the parameter D, providing the magnitude of the its axial component, and the angle θ between the metal-water molecule direction and the z axis of the ZFS frame. The variable-temperature relaxivity data for each isomer were fit to either an isotropic model (dashed lines) or an anisotropic model (solid lines), and the fits are displayed in Figure 6. Again although the quality of the isotropic fits was good, significant improvement in the high field region occurred after introduction of anisotropic motion.

The fitted parameters are listed in Table 5. There are several notable features contained in Table 5. First, in either the isotropic or anisotropic model, the fitted parameters for **A** and **B** are very similar within the model, with the exception of the water exchange parameters. This indicates that the differences in relaxation behavior can be solely attributed to differences in water exchange rates. In both models, electronic relaxation is relatively slow compared to values reported in the literature for similar GdDTPA derivatives.[17,19,28] The difference is in a much smaller value of Δ_t (about 3-fold smaller here). This is a benefit in that the relaxivity is higher as a consequence of slower electronic

(22) Caravan, P.; Astashkin, A. V.; Raitsimring, A. M. *Inorg. Chem.* **2003**, *42*, 3972−3974.
(23) Lipari, G.; Szabo, A. *J. Am. Chem. Soc.* **1982**, *104*, 4546−4559.
(24) Bertini, I.; Kowalewski, J.; Luchinat, C.; Nilsson, T.; Parigi, G. *J. Chem. Phys.* **1999**, *111*, 5795−5807.
(25) Kruk, D.; Nilsson, T.; Kowalewski, J. *PhysChemChemPhys* **2001**, *3*, 4907−4917.
(26) Bertini, I.; Luchinat, C.; Parigi, G. *Solution NMR of Paramagnetic Molecules*; Elsevier: Amsterdam, 2001.
(27) Kowalewski, J.; Luchinat, C.; Nilsson, T.; Parigi, G. *J. Phys. Chem. A* **2002**, *106*, 7376−7382.
(28) Vander Elst, L.; Maton, F.; Laurent, S.; Seghi, F.; Chapelle, F.; Muller, R. N. *Magn. Reson. Med.* **1997**, *38*, 604−614.

relaxation. Similarly small Δ_t values have also been obtained for other Gd complexes when bound to proteins[29,30] or liposomes.[31] There is no reason why Δ_t should become smaller when the complex associates with albumin. Indeed, a high-frequency EPR study of MS-325 in frozen solution in the presence of absence of HSA showed no difference in crystal-field parameters when MS-325 was bound to HSA.[32] This inconsistency probably arises from the use of approximate theories for the relaxivity of small complexes. In fact, the estimates of the larger Δ_t values came from studies on rapidly tumbling molecules, where the effect of the static ZFS is neglected. Actually, it has been shown that when the fast rotational motion is included as source of modulation of static ZFS, small Δ_t values are always obtained.[33] Furthermore, more thorough analyses of multifrequency EPR and NMRD of $[Gd(DTPA)(H_2O)]^{2-}$ which take static ZFS into account show lower values of Δ_t more in line with the values reported here.[34]

In the isotropic model, the water exchange parameters are different than those obtained by ^{17}O relaxation in the absence of HSA. This model suggests that upon binding to HSA at 35 °C, the water exchange rate for each isomer slows down (τ_m increases). However, the temperature dependence is also lower such that at 5 °C, the model suggests that the water exchange rate *speeds up* upon binding. It is difficult to conceive of a mechanism to explain this. On the other hand, the anisotropic model gives water exchange parameters very close to those obtained by ^{17}O NMR and suggests that there is no change in water exchange rates upon binding to albumin.

Comparing other parameters, one sees that there is a small change in the electronic parameters Δ_t and τ_v between the two models. The static zero-field splitting, *D*, is the same in both models, as is τ_R at 35 °C. However the temperature dependence of τ_R is significantly different.

In a previous paper,[35] the NMRD of the equilibrium mixture MS-325 was measured at 0.25 mM MS-325, 4% HSA, and 37 °C. Such data were analyzed using the Solomon−Bloembergen−Morgan equations and an isotropic model. The estimate of the rotational correlation time that was obtained is in good agreement with our analysis, and the water exchange rate was intermediate between the values obtained for each isomer using the isotropic model. Similar data (0.1 mM MS-325, 22.5% HSA, 37 °C),[6] collected and analyzed using the same model, provided again similar electronic best fit parameters (τ_m, Δ_t, τ_v), in good agreement with our analysis. The rotational correlation time in the latter case was about the double of the value obtained in the former case and in our fits. This is likely a consequence of the slower motion caused by the increased viscosity as a result of the increased protein concentration (22.5 vs 4.5%). In all analyses, the rotational correlation time was always much smaller than expected for a protein of the molecular size of HSA. As was previously noted,[35] this should be probably ascribed to some mobility freedom of the complex, which is not fully immobilized on the surface of the protein, and which should be taken into account, together with the faster motion on the picosecond time scale.

The concentrated protein data (0.1 mM MS-325, 22.5% HSA, 37 °C) were also analyzed using a model which includes a static ZFS modulated by the reorientation and a transient ZFS modeled using an anisotropic pseudorotation model.The parameters obtained in that analysis (including the electron relaxation parameters Δ_t and τ_v) are quite similar to the parameters here calculated using the isotropic model.

Finally, it is important to note that the conclusions of the initial study[6] still hold: the relaxivity increase in the presence of albumin is the result of a large increase in the rotational correlation time, coupled with a favorable water exchange rate; there is also a contribution from second-sphere relaxation.

Conclusion

The diastereomers of MS-325 have very similar properties with respect to their interaction with albumin. They bind with similar affinity and to the same region on albumin. When bound to albumin, the rotational dynamics and electronic structure of the complexes are the same. The major difference between the diastereomers is the water exchange rate. This differs by about a factor of 2 and impacts proton relaxation in the albumin bound case when the temperature is lowered. At physiological temperature, water exchange is not as limiting for relaxivity. The similar albumin-binding properties and similar albumin-bound relaxivities at 37 °C suggest that the efficacy of these interconverting diastereomers as MRI contrast agents is the same.

Acknowledgment. Thanks to Steve Witowski for assistance with some of the HPLC analyses.

IC700686K

(29) Anelli, P. L.; Bertini, I.; Fragai, M.; Lattuada, L.; Luchinat, C.; Parigi, G. *Eur. J. Inorg. Chem.* **2000**, 625−630.
(30) Bligh, S. W. A.; Chowdhury, A. H. M. S.; Kennedy, D.; Luchinat, C.; Parigi, G. *Magn. Reson. Med.* **1999**, *41*, 767−773.
(31) Alhaique, F.; Bertini, I.; Fragai, M.; Carafa, M.; Luchinat, C.; Parigi, G. *Inorg. Chim. Acta* **2002**, *331*, 151−157.
(32) Raitsimring, A. M.; Astashkin, A. V.; Poluektov, O. G.; Caravan, P. *Appl. Magn. Reson.* **2005**, *28*, 281−95.
(33) Kruk, D.; Kowalewski, J. *J. Magn. Reson.* **2003**, 229−40.
(34) Rast, S.; Fries, P. H.; Belorizky, E. *J. Chem. Phys.* **2000**, *113*, 8724−8735.
(35) Muller, R. N.; Radüchel, B.; Laurent, S.; Platzek, J.; Piérart, C.; Mareski, P.; Vander Elst, L. *Eur. J. Inorg. Chem.* **1999**, 1949−1955.
(36) Zhou, X.; Caravan, P.; Clarkson, R. B.; Westlund, P.-O. *J. Magn. Reson.* **2004**, *167*, 147−160.